

Eavesdropping on and Emulating MIFARE Ultralight and Classic Cards Using Software Defined Radio

Ilias Giechaskiel¹

Abstract

In this report, we describe a Software-Defined Radio (SDR) approach for eavesdropping on Near Field Communications (NFC) and Radio Frequency Identification (RFID) cards operating at 13.56 MHz. We show that GNU Radio and Python make a great platform for prototyping, while maintaining sufficient performance for passive attacks without extensive optimizations and using only modest processing power. We successfully eavesdrop on real MIFARE Ultralight and Classic 1K cards by capturing the raw radio waves with a home-made antenna. We recover the plaintext of both reader and tag fully by demodulating the incoming radio waves, parsing individual bits and error detection codes into packets, and then decrypting them when necessary. On the transmission side, we achieve full software emulation of the reader and of MIFARE Ultralight and Classic 1K cards (including encryption), and partial hardware emulation, where we correctly modulate the signal, but not within the strict timing limits of the protocol. Our transmissions can also be used to prevent legitimate communication by interfering with the intended reader or tag signals.

¹CDT in Cyber Security, University of Oxford, Oxford, United Kingdom

1. Introduction

Contactless cards and tags have become very popular in recent years, with everyday applications including e-passports [35], ticketing [37, 7, 12], access control [38], and payment [39, 11] systems. However, as these devices operate wirelessly, adversaries can pick up the radio signals and eavesdrop on the communication between a tag and a reader. Traditionally, such attacks on radio communications required dedicated hardware for particular frequencies and modulation types, but with the advent of Software-Defined Radio (SDR), it is possible to use generic equipment and perform the demodulation in software. Even so, despite a range of embedded devices and Field-Programmable Gate Arrays (FPGAs) that are capable of various attacks on Near Field Communication (NFC), Radio Frequency Identification (RFID), and related technologies (Section 2), to the best of our knowledge no open-source SDR implementation exists for High-Frequency (HF) NFC.¹

To this end, we developed such an implementation on an Ettus Research Universal Software Radio Peripheral (USRP) using Python and GNU Radio with an antenna made out of simple wire that allows passive eavesdropping on reader-tag communication (whose protocols are explained in Section 3). Though our implementation is easily extensible, we focused on MIFARE cards by NXP Semiconductors, since MIFARE has “a market share of more than 77% in the transport ticketing industry”, with “150 million reader and 10 billion contactless and dual interface IC’s sold” [26]. Specifically, we use Ultralight [30] and Classic 1K [28] cards, as the former does not employ any encryption, while the latter uses a bro-

ken cryptographic algorithm (Section 3.4), making them ideal candidates for such exploration. Moreover, we achieve full software and partial hardware reader and tag emulation, that can also be used to jam signals between a legitimate tag and reader. In summary, our contributions (detailed in Section 4 and evaluated in Section 5) are as follows:

1. We implement in pure Software-Defined Radio a demodulator for NFC/RFID readers and tags operating in the 13.56 MHz frequency, which decodes radio waves into plaintext packets.
2. We test our implementation by eavesdropping on real MIFARE Classic 1K and Ultralight communications with an RFID reader using a home-made antenna and a USRP, successfully decoding any encrypted packets.
3. We additionally implement in software the emulation of both readers and tags, including encryption if necessary.
4. Though our transmission capabilities cannot keep up with the NFC timing requirements, we show how our implementation can jam real reader-tag transmissions.
5. Overall, our work shows that prototyping using Software-Defined Radio is sufficient in practice for passive attacks, without the need for extensive optimizations or heavy computing power.

2. Related Work

Early work on RFID Hacking was conducted in a non-academic context, and focused on finding vulnerabilities in access control systems [33, 37]. Later, Buettner and Wetherall [5, 6, 4] experimented more systematically with RFID and SDR, but focused primarily on Gen 2 cards operating at 900 MHz. Their work was extended by others, typically in the context

¹Though they exist for UHF Gen2 cards. See <https://github.com/brunoprog64/rfid-gen2> and <https://github.com/yqzheng/usrp2reader> for instance.

of proposing better protocols [3, 41], but still for Ultra High Frequencies (UHF), with the exception of a recent work by Hassanieh et al. [14], which also included an extension to HF.

There have also been a number of designs which use microcontrollers and Field-Programmable Gate Arrays (FPGAs) for signal processing, such as the Proxmark 3 [40], RFIDler [22] and Chameleon [20]. Though such projects allow the use of custom firmware for additional functionality, they also require dedicated hardware in their design.

The MIFARE Classic cryptographic protocol was reverse-engineered by Nohl et al. by dissolving the plastic surrounding the chips, recovering the individual logic gates and converting them to a high-level algorithm [25]. Garcia et al. then discovered additional vulnerabilities of the protocol based on its nested authentication and parity bits [12]. Due to the wide range of applications of the MIFARE Classic, the topic became very popular for Master's thesis projects [34, 7, 32, 38], which found additional vulnerabilities, or examined the problem within the context of a specific application.

Finally, given the widespread availability of NFC-enabled mobile devices, researchers have also focused on NFC relay attacks using mobile phones [39, 11], as well as exploring [24] and protecting [13] the NFC mobile phone stack.

3. Background

The terms Radio Frequency Identification (RFID), Near Field Communication (NFC), contactless smartcards, proximity cards and vicinity cards are often used interchangeably, but they are covered by different standards and concern different parts of the radio spectrum. In this project, we looked at the ISO/IEC 14443 standard, with physical characteristics defined in [15], modulation and encoding in [17], initialization and anticollision in [18] and transmission protocols in [16].

Specifically, we focus on Type A communications, whose carrier frequency is $f_c = 13.56$ MHz. The reader – or Proximity Coupling Device (PCD) – communicates with the card – or Proximity Integrated Circuit Card (PICC) – through 100% Amplitude Shift Keying (ASK), with data using the Modified Miller encoding (Section 3.1). The communication from tag to reader utilizes Load Modulation with a subcarrier frequency of $f_s = f_c/16 = 847.5$ kHz, using Manchester encoding (Section 3.2), and both transmit at 106 kbit/s.

Because the carrier frequency is $f_c = 13.56$ MHz, the wavelength is $c/f_c \approx 22$ meters, making it impossible to deploy antennas that would fit in a card-size form-factor. Additionally, because the cards are passive (i.e. do not have their own power source), both the communication and the power source are achieved through inductive coupling from the PCD's antenna loop to the PICC's antenna loop. We discuss the high-level protocol in Section 3.3, and the MIFARE Classic encryption algorithm in Section 3.4.

3.1 PCD Transmissions

Amplitude Shift Keying (ASK) of depth $X\%$ is a form of digital modulation which specifies that if the amplitude of the

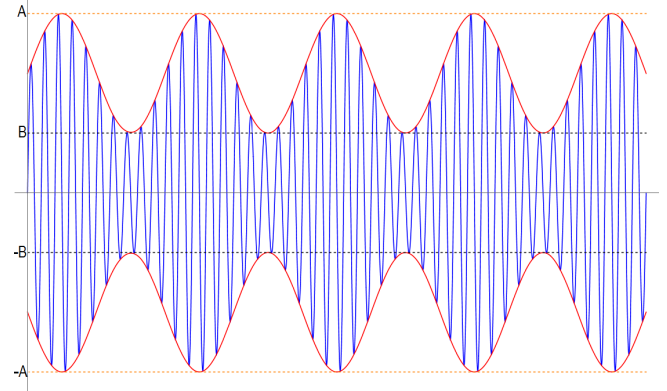


Figure 1. Amplitude Shift Keying (ASK) Peaks

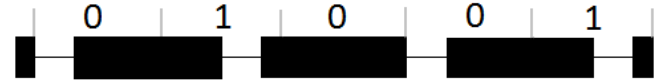


Figure 2. Modified Miller Encoding at 100% ASK

signal representing a digital 1 is equal to A and the amplitude of the signal representing a digital 0 is equal to B , then $X = \frac{A-B}{A+B}$ [1], as shown in Figure 1. Specifically, for 100% ASK, no signal is sent at all during a digital 0 (i.e. $B = 0$), indicating that such periods must be very brief, since the PICC needs to keep charge (using a capacitor) for the period of silence.

This is achieved through the Modified Miller Encoding, which ensures that there is no period of more than $3\mu s$ of silence (“pause”). Specifically, every bit is represented as a (combination of) signals lasting a total of $t_b = 128/f_c \approx 9.44\mu s$. The encoding (shown in Figure 2) is as follows:

- 1 is encoded as an unmodulated signal for $t_b/2 \approx 4.72\mu s$, followed by a period of silence for $3\mu s$, followed by an unmodulated signal for $t_b/2 - 3 \approx 1.72\mu s$
- 0 after a 0 is encoded as a silence period for $3\mu s$ followed by an unmodulated signal for $t_b - 3 \approx 6.44\mu s$
- 0 after a 1 is encoded as an unmodulated signal for a period of $t_b \approx 9.44\mu s$
- To indicate the beginning and the end of a transmission, a 0 bit is inserted at both the start and the end

In practice, however, because of hardware imperfections, the pause is not perfect, but needs to comply with the requirements shown in Figure 3. As a result, the modulated carrier for the encodings resembles Figure 4 which was recorded with our oscilloscope.

3.2 PICC Transmissions

As mentioned above, the tag does not have sufficient power for active transmissions. Consequently, the PICC achieves data transmission passively, by changing its *load*, which can be inferred as a voltage drop on the PCD, hence the term Load Modulation. Switching the load generates a subcarrier, which has a frequency $f_s = f_c/16 = 847.5$ kHz.

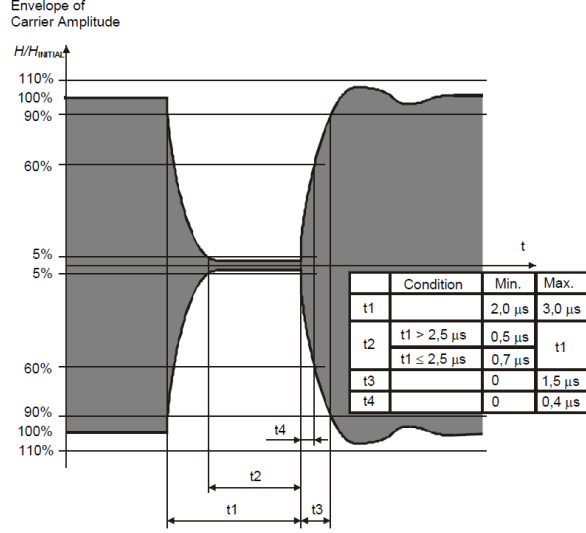


Figure 3. Miller Encoding Pause Requirements [17]

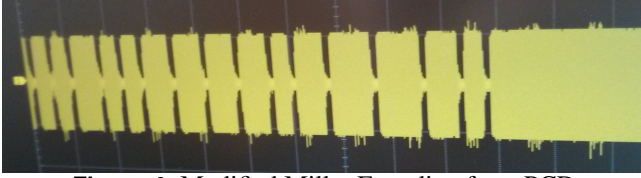


Figure 4. Modified Miller Encoding from PCD

The bits are then encoded using On-Off Keying (OOK) — or Manchester Encoding — as follows, with a total duration also equal to $t_b \approx 9.44\mu\text{s}$, which also equals 8 periods of the subcarrier, also shown in Figure 5:

- 1 is encoded by modulating the subcarrier for the *first* half ($= t_b/2 \approx 4.72\mu\text{s}$) of the bit duration
- 0 is encoded by modulating the subcarrier for the *second* half ($= t_b/2 \approx 4.72\mu\text{s}$) of the bit duration
- A logical 1 starts the transmission
- No modulation signifies the end of a transmission

3.3 The Protocol

Though the ISO/IEC 14443A protocol is general, we will focus on a few key aspects that are relevant to our discussion. As a result, we will refer the reader to [18] for more details such as timing requirements.

First of all, it is worth noting that each byte is ordered from the Least Significant Bit (LSB) to the Most Significant Bit (MSB), and that each byte is followed by an odd parity bit, meaning that an even number of high bits (ones) is followed by another high bit (one), whereas an odd number of ones is followed by a low bit (zero). For example, the byte 0x3F is encoded as 1111 1100 1.

The PCD signifies that it is waiting to read tags by repeatedly sending a REQA (0x26) or a WUPA (0x52), where the “A” signifies that type A protocol is used. The difference

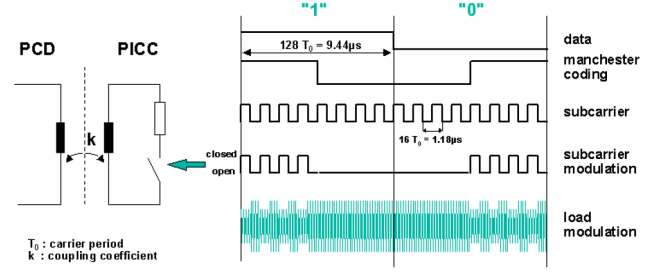


Figure 5. Manchester Encoding with Load Modulation [26]

between the REQA request and the WUPA wake-up request is that the latter also wakes up PICCs that were previously asked to HALT. Unlike all other commands, they are sent using a *short frame* that only consists of 7 bits, and which does not include a parity bit. As a result, the REQA command (including the beginning and end transmission zero bits) is sent as the sequence of bits 0 0110 010 0.

The standard has also defined Anticollision and Selection phases before the transmission of actual data which are used to ensure the non-interference from multiple tags and the correct selection of the tag. However, we only discuss them in the context of the MIFARE cards in Appendix A, since they are not necessary for understanding the rest of this report.

Finally, we mention that to detect errors with longer transmissions, for some requests and responses a Cyclic Redundancy Check (CRC) is used on the transmitted bytes (but excluding start/end and parity bits). The polynomial used is $x^{16} + x^{12} + x^5 + 1$, with a starting value of 0x6363, under the assumption that “FF0 shall be the leftmost flip-flop where data is shifted in [and] FF15 shall be the rightmost flip-flop where data is shifted out” [18]. For example, the HALT/HLTA command uses 2 bytes (0x50 0x00) followed by the two CRC bytes which can be calculated as 0x57 0xCD.

3.4 MIFARE Classic 1K Encryption

Even though the MIFARE Ultralight is ISO/IEC 14443 A compliant [30], the MIFARE Classic 1K uses a proprietary cryptographic protocol called CRYPTO1 [28]. The details of the protocol were not made publicly available, with the MIFARE datasheets only broadly explaining the 3-pass protocol [28]. Each sector (equal to 4 blocks of 16 bytes each) has two 6-byte keys (Key A and B), which on delivery are set to [0xFF 0xFF 0xFF 0xFF 0xFF 0xFF] (but can be changed later on a per-sector basis). Each authentication happens with one of the two keys chosen by the reader, and can only be used to access a specific sector. Each sector contains one block (the sector trailer) which contains the two keys and some access bits which determine the allowed operations for the 4 blocks (See Appendix A.2 for more details).

The PCD indicates to the PICC that it wants to authenticate through a command indicating which key to be used and what address to use. As shown in Figure 6, the three-pass scheme consists of a 4 byte challenge sent from the PICC to the PCD (Token RB), an 8-byte challenge and response (of 4

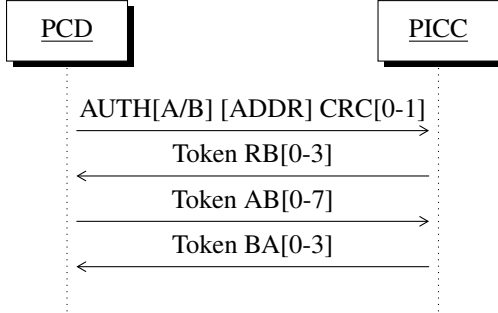


Figure 6. MIFARE Classic Authentication Protocol

bytes each) send from the PCD to the PICC (Token AB) and a response from the PICC to the PCD (Token BA), if the reader’s encryption was correct. After the first challenge (Token RB), **all** traffic is encrypted, even subsequent authentications, which leads to a weakness known as nested authentication [12].

Though we discuss the encryption algorithm in greater detail in Appendix B, it is worth noting a few things based on the research in [25, 12]. The CRYPTO1 encryption scheme is a stream cipher which consists of a 48-bit (equal to the key length) Linear Feedback Shift Register (LFSR) and a non-linear filter function [25]. The encryption incorporates both the tag’s Unique Identifier (UID) and the random nonce RB, which however is only generated using a 16-bit LFSR. Nonetheless, both challenge responses only depend on the tag’s nonce (and not the reader’s nonce or the UID), and use the same LFSR as the Random Number Generator (RNG).

What is more, the parity bits are also encrypted (making the MIFARE Classic 1K *incompatible* with the ISO 14443 protocol), and “the bit of keystream used to encrypt the parity bits is reused to encrypt the next bit of plaintext” [12]. This vulnerability, in combination with the nested authentication mentioned above (which causes the token RB to also be encrypted) leaks data which can be used to guess the nonce or to reveal the secret key.

4. Implementation

In this section we discuss our setup and methodology (Section 4.1), the design of the antenna (Section 4.2), as well as our approach for decoding transmissions (Section 4.3) and for emulating them (Section 4.4).

4.1 Setup and Methodology

For this project, we use Ettus Research’s Universal Software Radio Peripheral (USRP) N210 [10], in combination with the BasicRX/TX and LFRX/TX daughterboards [9], both of which cover 13.56 MHz. The USRP has become the de-facto SDR platform, and also allows custom code to be written on its FPGA, which we did not pursue in this project. Instead, all signal processing is done on a laptop, using Python and the GNU Radio toolkit/framework, which is easily extensible and provides many building blocks (“modules”) that can be incorporated into new designs.

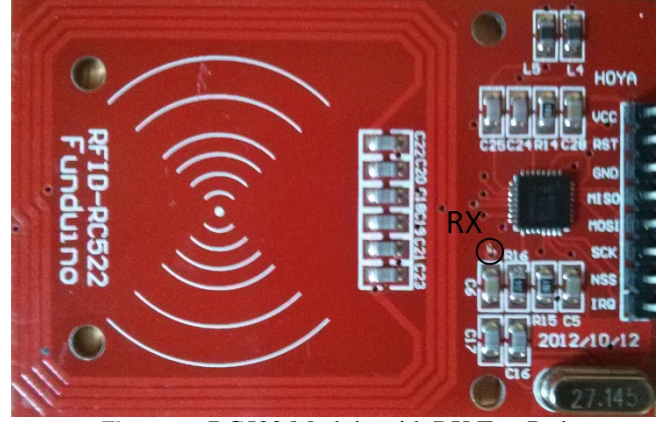


Figure 7. RC522 Module with RX Test Pad

The laptop used is a Samsung NP900X4C with an Intel i5-3317U @ 1.7 GHz and 8 GB of RAM, but the operating system (Kali Linux 1.1.0a) is booted off a 16 GB USB 3.0 Lexar JumpDrive. Moreover, due to the lack of an Ethernet port, the USRP is connected to the laptop on a Plugable USB3-E1000 USB 3.0 Gigabit Ethernet Adapter.

To measure signals accurately, we use a Rigol DS2302A digital oscilloscope with two 300 MHz channels [36]. The actual PCD is an RFID-RC522 module using the MFRC522 chip by NXP Semiconductors [31] connected to an Arduino UNO using the Serial Peripheral Interface (SPI) and the DumpInfo example at [2]. Figure 7 shows the module along with the highlighted test pad for the reception (RX) part of the antenna, which was connected to the oscilloscope to test reception.

The types of cards used are Classic 1Ks and NTAG203s [29], which are compatible with the Ultralight. The NTAG203 is actually larger and has a different memory layout, but the Arduino library does not distinguish between the two, so only 16 out of 42 pages are revealed. It is important to note that although we only use two *types* of cards, more than one actual card per type is tried with identical results.

4.2 The Antenna

Much research has been conducted into making RFID-type antennas work well and up to a large distance, with much of it available as application notes [26, 23, 27]. Many of them are also available for direct purchase, such as the DLP-RFID-ANT by DLP Design,² but fundamentally the RFID antenna is just an inductor, made out of wire wrapped into a coil. These home-made antennas made out of simple wire (or out of NFC tags [21]) have proven themselves to work [8], so we make our own. Specifically according to [27], the inductance should be between 300 nH and 3 μ H, so using Equation (1) with $N = 8$ turns, $D = 4$ cm, and $s = 2.8$ mm (22 AWG), we get an inductance of 5.28 μ H, which is within the prescribed limits.

$$L[nH] = \frac{24.6 \cdot N^2 \cdot D[cm]}{1 + 2.75 \cdot \frac{s[cm]}{D[cm]}} \quad (1)$$

²Found at <http://www.dlpdesign.com/rf/ant1.shtml>

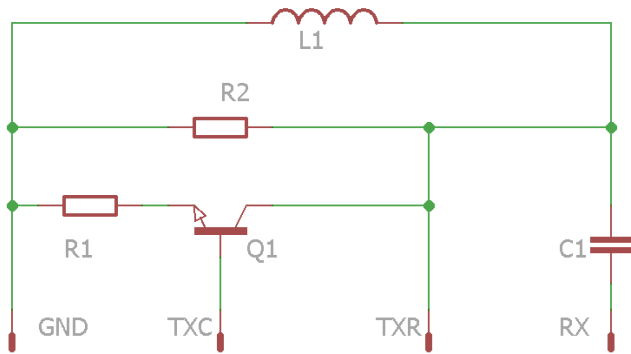


Figure 8. Antenna Schematic for RX and TX (Card/Reader)

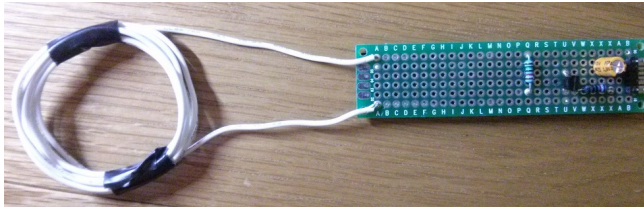


Figure 9. Final Antenna PCB

The signal strengths of the wire loop and of the RC522 RX test pad directly are approximately equal when they are less about a cm apart, but connecting our antenna to the USRP results in a considerable signal strength drop, and requires a tuning capacitor in series with the antenna. For emulating PICC transmissions (TX) through Load Modulation, we use a transistor and 2 resistors. Their values are empirically determined, but the high-level schematic is included in Figure 8, with the final circuit in Figure 9.

Though we discuss the antenna more in Section 5, we mention that the range for eavesdropping on both reader and tag is only about 1-2 cm. To remedy this, we tape the antenna to the back of the RC522 reader, and the tag to be read to the front of it as shown in Figure 10.

4.3 Eavesdropping

For consistency/determinism, and easy testing/reproducibility, we record the interaction between the reader and the tag. This is achieved by using our home-made antenna connected to the USRP in the setup of Figure 10. The *envelope* of the signal is sufficient for our purposes, and for our Amplitude Modulated (AM) signal can be calculated as the absolute value of the signal. Recoding the envelope as a WAV file (using GNU Radio's `wavfile_sink`) using a sample rate of 2,000,000 samples/second and a 16-bit output, results in 4 MB of data to be processed per second.

Opening the resulting audio file in Audacity Audio Editor, we see that for PCD transmissions the signal drops close to 0, while for PICC transmissions the subcarrier spikes hover at about 5-10% above the average. An annotated example of the REQA and ATQA transmissions is shown in Figure 11, where start/end and parity bits are shown in red.

Consequently, we can detect such transitions by having a

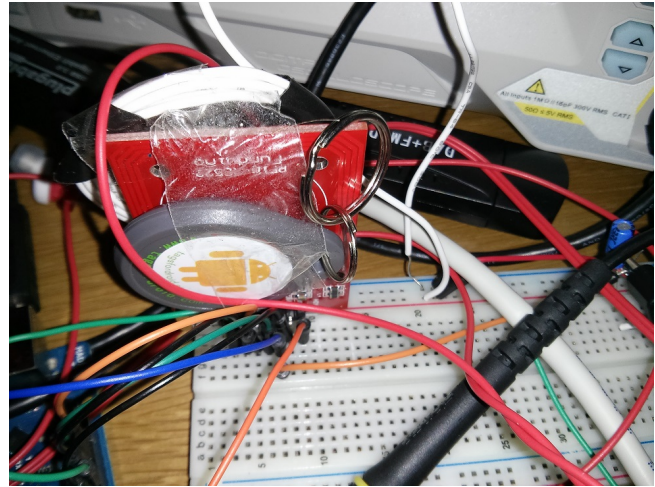


Figure 10. Setup: PICC and Antenna Attached to PCD

moving window (say of length 2,000) that keeps track of the average, and if the next value is below the *low* threshold (10% of the average), it is considered part of the reader transmission, and if it goes above the *high* threshold (110% of the average), a part of the card transmission. The transmission is considered over when the signal has returned to its average values for too long (currently $> 25\mu s$), and to ensure that the average does not drift, values above the high threshold and below the low threshold are not included in the moving average. The duration and values of these transitions are then passed on to the appropriate decoders through callbacks, so that the decoding runs in a background thread.

The two decoders (one for Manchester Encoding, and the other for the Modified Miller Encoding) are essentially Finite State Machines (FSM) that implement the specifications mentioned in Sections 3.1 and 3.2, allowing for some margin of transmission and measurement errors. For instance, the sequence $[(0, 3), (1, 11), (0, 3), (1, 16), (0, 3), (1, 6)]$ of PCD (bit, μs duration) pairs would be (approximately) split as:

$$\begin{aligned} [(0, 3), (1, 6.5)] &\rightarrow 0 \\ [(1, 4.5), (0, 3), (1, 1.5)] &\rightarrow 1 \\ [(1, 9.5)] &\rightarrow 0 \\ [(1, 5), (0, 3), (1, 1.5)] &\rightarrow 1 \\ (1, 4.5) &\rightarrow \text{state}=\text{ONE_FIRST_STAGE} \end{aligned}$$

Having recovered all the bits (including parity, but discarding any start/end bits), and knowing whether the PCD or the PICC is doing the transmission, these bits can be interpreted with context in a more high-level FSM. This is the code that updates the internal state of the tag/reader when needed (e.g. to decrypt bits in the MIFARE Classic case), ensures that the parity is correct and transforms bits into bytes, and then based on the current state and the “header” of the incoming bytes determines the command issued, interprets the bytes and checks any CRC if necessary.

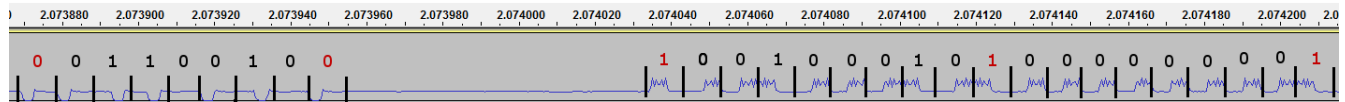


Figure 11. Annotated Recoding of PCD (REQA) and PICC (ATQA) Transmissions. Start/End/Parity Bits Shown in Red

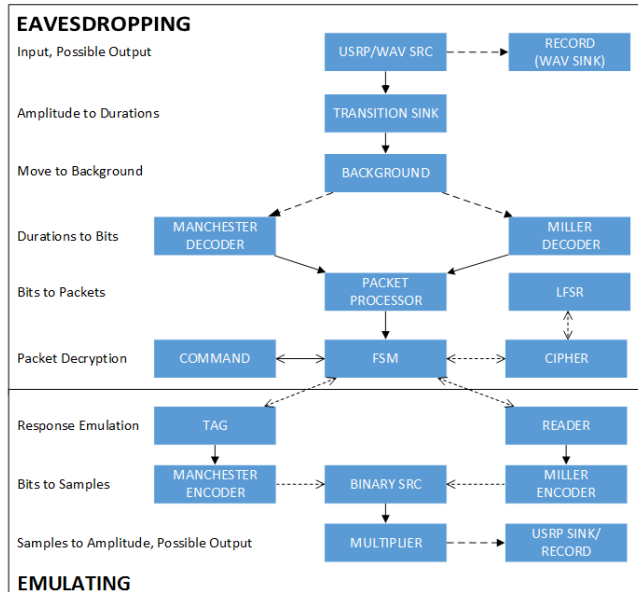


Figure 12. High-Level Code Overview. Lines Represent Information Flow, with Dashes Being Optional

For unencrypted commands, this process is not crucial,³ but for the Classic 1K, parsing the commands to get the UID, for instance, is of utmost importance as any deviations would result in ciphertext that cannot be decrypted. Specifically for regular data transmission decryption is straightforward, but the setup phase of the challenge-response protocol needs to be handled more subtly, especially because of nested authentications after the first authentication. Hence, while the actual cipher is abstracted away into a different class, it is the responsibility of the FSM to correctly call it.

A (simplified) high-level overview of the eavesdropping code is found in the top of Figure 12 summarizing our previous discussion: the audio/USRP source is passed to a “transition sink” which detects amplitude transitions and passes them to a background thread which dispatches the Manchester and Miller decoders turning transitions into bits. These bits are then converted into packets, and are passed to the FSM which deciphers them and decodes them into MIFARE commands.

4.4 Emulating

The FSM is also crucial for the PCD and PICC emulation, since it centralizes all encryption considerations. As a result, the emulated Reader and Tag only deal with plaintext messages (and not individual bits). Specifically, the Reader is set to perform identically to the Arduino `DumpInfo` program, by performing the anticollision, and then reading all

card blocks. The Tag is programmed to respond to the incoming commands, and its memory layout is set dynamically through files. For reproducibility (and especially when emulating against a recording), the Tag and Reader randomness can also be fixed, but it can also be generated on-the-fly as needed, ensuring that this is not merely a replay attack.

Because of this setup, it is possible to emulate both the reader and the tag simultaneously, without needing to go through encoding and modulation, but we have also coded the Manchester and Modified Miller encodings (in a reverse fashion to Section 4.3), as well as modulation, so that they can be output to a WAV file for use without a USRP.

Modulating the Reader’s output is straightforward: it is enough to generate a 13.56 MHz (sine wave) carrier and output it, or output nothing for the “pause” duration. Load Modulation of the Tag is more complicated, and is achieved by only outputting when the encoding is a logical 1 (for either $4.5\mu s$ or $9\mu s$). Specifically, however, and as explained in Section 3.2 (Figure 5), this is achieved by generating a 847.5 kHz subcarrier, multiplying by the bit to output, and then switching the load (in this case through the transistor) only for the amount of time for which the signal is positive.

The simplified high-level overview of the emulation code can be found in the bottom of Figure 12. After the eavesdropping code has decoded incoming transmission, the FSM passes the commands to the Tag and/or Reader which determine the suitable response and pass it back to the FSM. If the command is to be output somewhere, it is Manchester/Miller encoded, and then passed on to a block which converts bit durations into samples. These samples are then modulated with the suitable carrier and output into a WAV file/the USRP.

5. Evaluation

In this section, we take a critical look at our approach for eavesdropping (Section 5.1) and for emulating (Section 5.2).

5.1 Eavesdropping

First of all, it is worth mentioning that with recorded reader-tag communications, the eavesdropping code behaves predictably and always correctly decodes the messages, and sample traces are included in Appendix C. However, at least initially, the code required 50 seconds of processing per 1 second of data. This was due to the fact that incoming messages in GNU Radio Python code are stored as NumPy arrays which do not support efficient iteration. Converting them to a list before iteration resulted in a $10\times$ improvement, and assigning local names to function calls resulted in an additional $2.5\times$ improvement, for a processing cost of about 2.2 seconds per 1 second of data. This is still not real time, but given the unusual

³The code will just print the plaintext bytes for unknown commands.



Figure 13. Signal Received with Fixed Tag and Arduino Reset: PICC (PCD) Transmissions Above (Below) the Average



Figure 14. Signal Received when Approaching Tag: Weak (Close to Average) PICC Transmissions

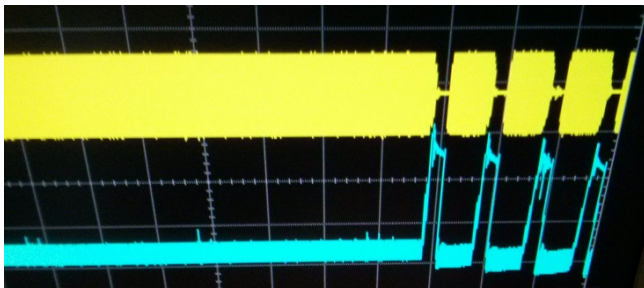


Figure 15. Amplification: Original (Top), Distorted (Bottom)

setup which relies heavily on the USB bus, this performance is acceptable given the convenience of prototyping in Python.

Moreover, even if the logic for tags other than the MIFARE Classic and Ultralight has not been implemented, the demodulation still works, and if the transmissions are not encrypted, the code will still be able to dump the plaintext (un-interpreted) bytes. What is more, the moving average methodology of detecting amplitude deviations and distinguishing between PCD and PICC transmissions works well — even when there are sudden changes to the average. For example, pressing the reset button in the Arduino results in a sudden and prolonged signal loss (Figure 13), but the code can still recover all transmissions that follow.

This remains true even when testing a more “real-world” situation, where the user approaches the reader with the tag (Figure 14). As can be seen, the signal strength drops when the tag starts approaching the reader (due to their coupling), and initially the signal strength of the PICC transmissions is not sufficient for recovery. In this case, the code can recover all PCD transmissions, but only the PICC transmissions after the first READ request.

As this experiment shows, though successful, the setup could have substantially benefited from a more fine-tuned antenna with a longer range and better shielding. It is worth mentioning that we also attempted to create an HF amplifier based on the design in [19] with a couple of minor resistance modifications to make it work with 9V, but the modifications resulted in the signal distortion shown in Figure 15.

5.2 Emulating

The code makes it possible to simultaneously emulate both reader and tag without any external input — and produce traces identical to those of real eavesdropping. Testing the

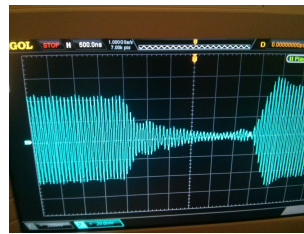


Figure 16. Emulated Signal

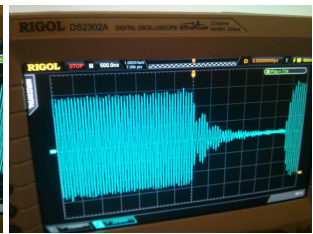


Figure 17. Real Signal



Figure 18. Reader TX in Yellow, RC522 Antenna in Blue

software emulation against a recording is somewhat more complicated, but relies on the code overview of Figure 12. For example, to test the PICC emulation, the eavesdropper decodes PCD commands and passes them on to the emulator, which produces the responses and also saves their modulation to a WAV file (at twice the sampling rate). We manually compare the emulated responses to the expected (real) responses, and also run our WAV file against the eavesdropper, ensuring that transmissions can be demodulated correctly.

However, due to the lack of real-time signal processing, testing the transmissions against real hardware is challenging as the emulation does not adhere to the strict ISO and MIFARE timing requirements. However, we focus on the produced waveforms as measured by our oscilloscope at both the USRP output, and at the RC522 Antenna (which is used as a proxy for what a real PCD/PICC device would be receiving).

Figure 16 shows the USRP’s emulated PCD signal, while Figure 17 shows a real signal transmitted (independently) by the RC522. As we can see, the two waveforms look very similar, and indeed the emulated signal seems to adhere to the pause requirements of Figure 3, indicating that Reader



Figure 19. Tag TX in Yellow, RC522 Antenna in Blue

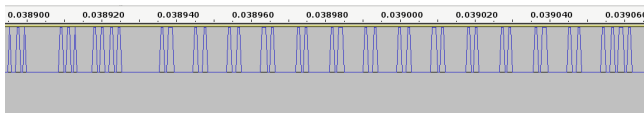


Figure 20. Load Modulation Before TX

Emulation works in principle. Of course, as shown in Figure 18, the USRP signal is not particularly strong (yellow), and the reception on the (unpowered) RC522 antenna (blue) already indicates a strength drop due to our untuned transmissions.

The implementation of the hardware tag emulation was not as successful. Specifically, even with the LFTX daughterboard, we could not get any signal transmission out of the USRP at the 847.5 kHz range, so the “subcarrier” used is 13.56 MHz. The behavior of the signal strength is similar (Figure 19), but it is unclear why the signal exiting the USRP is alternating. Specifically, as explained in Section 4.4, in order to simulate load modulation, we essentially switch on and off a transistor, so the signal existing the USRP is supposed to be non-negative, as we verified by the WAV output (Figure 20). This, however, does not seem to be the case when testing the output at the USRP.

Even so, our implementation can be used to jam signals by transmitting at the same time as a real transmission (Figure 21). This way we can (dynamically) interfere with transmissions (although with some processing lag), resulting in timeouts and other errors at the Arduino end.

6. Conclusions and Future Work

All in all, the Software-Defined Radio (SDR) approach for eavesdropping and emulating MIFARE Classic 1K and Ultralight cards proved to be very fruitful for an initial exploration and prototyping phase. The approach of the moving average window works well even with varying signal strength, and overall both encoding and decoding, as well as modulating and demodulating are functionally complete. Moreover, the code is modular and easily extensible and works even with unknown commands (provided they are not encrypted). What is more, full software and partial hardware emulation was achieved, which was sufficient to prevent legitimate PCD-PICC communications. Finally, performance was adequate

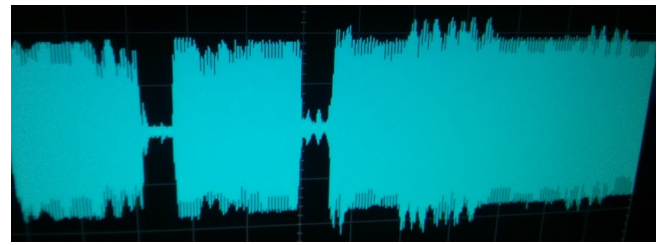


Figure 21. Tag TX Overlap with RC522 Reader

for non-real-time processing without any extensive optimizations and with only a modest setup, which presents a great performance-complexity trade-off.

As a result, future work could focus on comparing the SDR approach with embedded platforms (C++ or FPGA), which would presumably yield better results (especially for higher sampling rates), but at the cost of additional development investment. Moreover, new experiments could focus on achieving the timing requirements of the protocol — for instance through clock recovery for synchronization and with better antennas — and looking at newer cards such as the MIFARE Ultralight EV1 and DESFire EV2, but we firmly believe that this work is a good start towards such goals.

Acknowledgments

I would like to thank Kasper Rasmussen for being my supervisor, for his invaluable help throughout the project, for his comments on earlier versions of this report, and for entrusting me with his expensive equipment. I would also like to thank Simon Crowe for helping shape the focus of the project. Finally, I would like to thank Kellogg College and their Research Support Grant which enabled the purchase of some of the components that were used in this project.

References

- [1] ATMEL. *Understanding the Requirements of ISO/IEC 14443 for Type B Proximity Contactless Identification Card*, 11 2005.
- [2] BALBOA, M. Arduino RFID library for MFRC522. <https://github.com/miguelbalboa/rfid>. Acc.: 2015-06-19.
- [3] BRIAND, A., ALBERT, B., AND GURJAO, E. Complete software defined RFID system using GNU radio. In *IEEE International Conference on RFID-Technologies and Applications (RFID-TA 2012)*.
- [4] BUETTNER, M., AND WETHERALL, D. A software radio-based UHF RFID reader for PHY/MAC experimentation. In *IEEE International Conference on RFID 2011*.
- [5] BUETTNER, M., AND WETHERALL, D. A flexible software radio transceiver for UHF RFID experimentation. Tech. Rep. UW-CSE-09-10-02, University of Washington - Computer Science Department, 2009.

- [6] BUETTNER, M., AND WETHERALL, D. A "Gen 2" RFID monitor based on the USRP. *SIGCOMM Comput. Commun. Rev.* (2010).
- [7] DE KONING GANS, G. Analysis of the MIFARE classic used in the OV-Chipkaart project. Master's thesis, Radboud University Nijmegen, 2008.
- [8] DIAKOS, T., BRIFFA, J., BROWN, T., AND WESEMEYER, S. Eavesdropping near field contactless payments: A quantitative analysis. *IET Jour. of Eng.* (2013).
- [9] ETTUS RESEARCH. *TX and RX Daughterboards For the USRP Software Radio System*.
- [10] ETTUS RESEARCH. *USRP N200/N210 Networked Series*.
- [11] FRANCIS, L., HANCKE, G., MAYES, K., AND MARKANTONAKIS, K. *Practical Relay Attack on Contactless Transactions by Using NFC Mobile Phones*.
- [12] GARCIA, F. D., ROSSUM, P. V., VERDULT, R., AND SCHREUR, R. W. Wirelessly pickpocketing a Mifare Classic card. In *Proceedings of the 30th IEEE Symposium on Security and Privacy (SSP 2009)*.
- [13] GUMMESON, J. J., PRIYANTHA, B., GANESAN, D., THRASHER, D., AND ZHANG, P. Engarde: Protecting the mobile phone from malicious nfc interactions. In *11th Annual International Conference on Mobile Systems, Applications, and Services (MobiSys 2013)*.
- [14] HASSANIEH, H., WANG, J., KATABI, D., AND KOHNO, T. Securing RFIDs by randomizing the modulation and channel. In *12th USENIX Symposium on Networked Systems Design and Implementation (NSDI 2015)*.
- [15] ISO. Identification cards—Contactless integrated circuit cards—Proximity cards—Part 1: Physical characteristics. ISO 144443-1:2008, International Organization for Standardization, 2008.
- [16] ISO. Identification cards—Contactless integrated circuit cards—Proximity cards—Part 4: Transmission protocol. ISO 144443-4:2008, International Organization for Standardization, 2008.
- [17] ISO. Identification cards—Contactless integrated circuit cards—Proximity cards—Part 2: Radio frequency power and signal interface. ISO 144443-2:2010, International Organization for Standardization, 2010.
- [18] ISO. Identification cards—Contactless integrated circuit cards—Proximity cards—Part 3: Initialization and anti-collision. ISO 144443-3:2011, International Organization for Standardization, 2011.
- [19] JENKINS, M. A signal amplifier module for HF. <http://marcusjenkins.com/amateur-radio-2/a-signal-amplifier-module-for-hf/>. Acc.: 2015-06-19.
- [20] KASPER, T., VON MAURICH, I., OSWALD, D., AND PAAR, C. Chameleon: A versatile emulator for contactless smartcards. In *Information Security and Cryptology (ICISC 2010)*.
- [21] KORTVEDT, H. Eavesdropping near field communication. In *NISK 2009*.
- [22] LAURIE, A. RFIDler. <https://github.com/ApertureLabsLtd/RFIDler>. Acc.: 2015-06-19.
- [23] MICROCHIP. *Antenna Circuit Design for RFID Applications*, 2003.
- [24] MILLER, C. Exploring the NFC attack surface. Presented at Black Hat USA 2012.
- [25] NOHL, K., EVANS, D., STARBUG, S., AND PLÖTZ, H. Reverse-engineering a cryptographic RFID tag. In *Proceedings of the 17th Conference on Security Symposium (USENIX Security 2008)*.
- [26] NXP SEMICONDUCTORS. About MIFARE. <https://www.mifare.net/en/about-mifare/>. Acc.: 2015-06-19.
- [27] NXP SEMICONDUCTORS. *Antenna design guide for MFR52x, PN51x and PN53x*, 10 2010. Rev. 1.2.
- [28] NXP SEMICONDUCTORS. *MIFARE Classic 1K - Mainstream contactless smart card IC for fast and easy solution development*, 2 2011. Rev. 3.1.
- [29] NXP SEMICONDUCTORS. *NFC Forum Type 2 Tag compliant IC with 144 bytes user memory*, 2011. Rev. 3.2.
- [30] NXP SEMICONDUCTORS. *MIFARE Ultralight contactless single-ticket IC*, 7 2014. Rev. 3.9.
- [31] NXP SEMICONDUCTORS. *Standard 3V MIFARE reader solution*, 9 2014. Rev. 3.8.
- [32] PENRI-WILLIAMS, K. E. Implementing an RFID 'Mifare Classic' attack. Master's thesis, City University London, 2009.
- [33] PLÖTZ, H. RFID hacking. Presented at the 23rd Chaos Communication Congress (CCC 2006).
- [34] PLÖTZ, H. Mifare classic – eine analyse der implementierung. Master's thesis, Humboldt-Universität, 2008.
- [35] RICHTER, H., MOSTOWSKI, W., AND POLL, E. Fingerprinting passports. NLUUG spring conference on security (2008).
- [36] RIGOL TECHNOLOGIES, INC. *MSO/DS2000A Series Digital Oscilloscope*.
- [37] RYAN, R., ANDERSON, Z., AND CHIESA, A. Anatomy of a subway hack. Presented at the 16th DEFCON Hacking Conference (DEFCON 2008).
- [38] TAN, W. H. Practical attacks on the MIFARE Classic. Master's thesis, Imperial College London, 2009.
- [39] WEISS, M. Performing relay attacks on ISO 14443 contactless smart cards using NFC mobile equipment. Master's thesis, Technischen Universität München, 2010.
- [40] WESTHUES, J. Proxmark 3. <https://github.com/Proxmark/proxmark3>. Acc.: 2015-06-19.
- [41] ZHENG, Y., AND LI, M. ZOE: Fast cardinality estimation for large-scale RFID systems. In *INFOCOM* (2013).

Appendices

A MIFARE Cards

In this section, we discuss the memory layout and commands used by the MIFARE Ultralight (Section A.1) and Classic 1K cards (Section A.2) based on their datasheets [30, 28], with more general ISO details in [18].

A.1 MIFARE Ultralight

As shown in Table 1, the MIFARE Ultralight has a 7-byte UID SN[0-6], including 2 check bytes BCC[0-1]. SN0 is the manufacturer ID (0x04 for NXP Semiconductors), and the check bytes are defined as follows: $BCC0 = 0x88 \oplus SN0 \oplus SN1 \oplus SN2$ and $BCC1 = SN3 \oplus SN4 \oplus SN5 \oplus SN6$. Lock bytes can be used to turn pages into read-only mode, while One-Time Pad (OTP) bytes can be set to 1, but never set back to 0 again. Table 2 shows the possible commands when communicating with a MIFARE Ultralight card. The address for the READ and WRITE commands are between 0x00 and 0x0F and include roll-over, while C[0-1] is the CRC, and D[0-15] refer to data bytes. The full FSM can be seen in Figure 22.

Table 1. MIFARE Ultralight Memory Layout

| Page Address | 4 Byte Contents |
|--------------|--------------------------------------|
| 0x00-0x01 | Serial Number |
| 0x02 | [SN, Internal, Lock Byte, Lock Byte] |
| 0x03 | One Time Pad |
| 0x04-0x0F | User Memory |

Table 2. MIFARE Ultralight Commands

| Command | Code | Response |
|-------------------------|---------------------------------------|-----------------------|
| REQA | 0x26 | 0x44 0x00 (ATQA) |
| WUPA | 0x52 | 0x44 0x00 (ATQA) |
| ANTICOLLISION (1) | 0x93 0x[20-67] | 0x88 SN0 SN1 SN2 BCC0 |
| SELECT (1) | 0x93 0x70 0x88 SN0 SN1 SN2 BCC0 C0 C1 | 0x04 C0 C1 |
| ANTICOLLISION (2) | 0x95 0x[20-67] | SN3 SN4 SN5 SN6 BCC1 |
| SELECT (2) | 0x95 0x70 SN3 SN4 SN5 SN6 BCC1 C0 C1 | 0x00 C0 C1 |
| READ | 0x30 [Addr] C0 C1 | D0 D1 ... D15 C0 C1 |
| WRITE | 0xA2 [Addr] D0 D1 D2 D3 C0 C1 | [ACK/NAK] |
| COMPATIBILITY WRITE (1) | 0xA0 [Addr] C0 C1 | [ACK/NAK] |
| COMPATIBILITY WRITE (2) | D0 D1 ... D15 C0 C1 | [ACK/NAK] |
| HALT | 0x50 0x00 C0 C1 | [Passive ACK/NAK] |

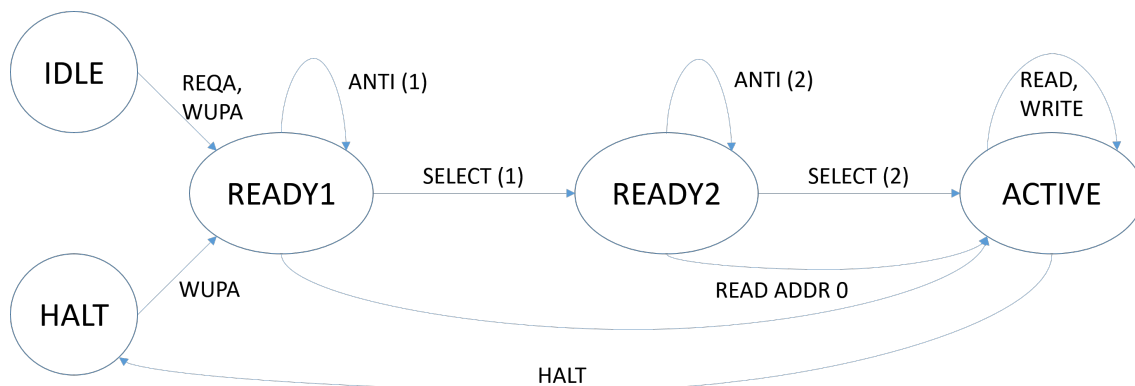


Figure 22. MIFARE Ultralight FSM

A.2 MIFARE Classic 1K

As indicated in Figure 23, the Classic 1K only uses a single round of ANTICOLLISION and SELECT commands, but includes a much more complicated 3-pass authentication mechanism. We explain in detail the encryption scheme in Appendix B, but we focus on the card's memory layout, which is summarized in Table 3. The card does not have a globally-unique identifier, but instead uses a 4-byte Non-Unique Identifier (NUID) in block 0. Each sector has a block called the “trailer”, which contains the two keys and the access bits. The layout for these access bits is shown in Table 5, where CX_y is the X 'th access bit for block y . These access bits are interpreted differently based on whether the block is a trailer block or a data block (Table 5). It is worth noting that the data blocks can be used for simple read/write operations, or they can be used as “value blocks” for applications which need more robustness and backups and could benefit from operations like INCREMENT and DECREMENT.

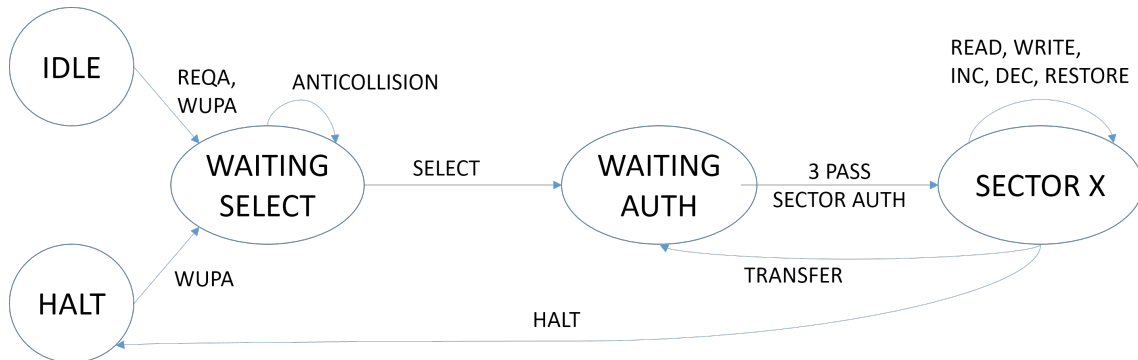


Figure 23. Classic 1K FSM

Table 3. MIFARE Classic 1K Memory Layout

| Sector | Block | 16 Byte Contents |
|--------|---------------|---|
| [0-15] | [0-2] | User Data Manufacturer Data in Sector 0, Block 0 |
| [0-15] | 3 (“Trailer”) | Key A (6 Bytes), Access Bits (4 Bytes), Key B (6 Bytes) |

Table 4. Access Bits Layouts

| Byte \ Bit | 7 | 6 | 5 | 4 | 3 | 2 | 1 | 0 |
|------------|-------------------|-------------------|-------------------|-------------------|-------------------|-------------------|-------------------|-------------------|
| 6 | $\overline{C2_3}$ | $\overline{C2_2}$ | $\overline{C2_1}$ | $\overline{C2_0}$ | $\overline{C1_3}$ | $\overline{C1_2}$ | $\overline{C1_1}$ | $\overline{C1_0}$ |
| 7 | $C1_3$ | $C1_2$ | $C1_1$ | $C1_0$ | $\overline{C3_3}$ | $\overline{C3_2}$ | $\overline{C3_1}$ | $\overline{C3_0}$ |
| 8 | $C3_3$ | $C3_2$ | $C3_1$ | $C3_0$ | $C2_3$ | $C2_2$ | $C2_1$ | $C2_0$ |
| 9 | User Data | | | | | | | |

Table 5. Read (R), Write (W), Increment (I) and Decrement/Transfer/Restore (O) Access Matrix

| Access Bits | Trailer Block | | | Data Block | |
|-------------|---------------|---------------|--------|---------------|------------------|
| C[1-3] | Key A | Access Bits | Key B | Read/Write | Increment/Others |
| 000 | W (A) | R (A) | RW (A) | RW (A, B) | IO (A, B) |
| 001 | W (A) | RW (A) | RW (A) | R (A, B) | O (A, B) |
| 010 | - | R (A) | R (A) | R (A, B) | - |
| 011 | W (B) | R (A), RW (B) | W (B) | RW (B) | - |
| 100 | W (B) | R (A, B) | W (B) | R (A), RW (B) | - |
| 101 | - | R (A), RW (B) | - | R (B) | - |
| 110 | - | R (A, B) | - | R (A), RW (B) | O (A), IO (B) |
| 111 | - | R (A, B) | - | - | - |

Table 6 presents the commands recognized by Classic 1K cards, where $NID[0-3]$ represents the NUID and $BCC = NID0 \oplus NID1 \oplus NID2 \oplus NID3$. Addresses range from 0x00 to 0x3F, while $C[0-1]$ refers to the Checksum and $D[0-15]$ to data bytes.

Table 6. MIFARE Classic 1K Plaintext Commands

| Command | Code | Response |
|------------------|---|-------------------------|
| REQA | 0x26 | 0x04 0x00 (ATQA) |
| WUPA | 0x52 | 0x04 0x00 (ATQA) |
| ANTICOLLISION | 0x93 0x20 | NID0 NID1 NID2 NID3 BCC |
| SELECT | 0x93 0x70 NID0 NID1 NID2 NID3 BCC C0 C1 | 0x08 C0 C1 |
| AUTHA | 0x60 [Addr] C0 C1 | D0 D1 D2 D3 [TOKEN RB] |
| AUTHB | 0x61 [Addr] C0 C1 | D0 D1 D2 D3 [TOKEN RB] |
| AUTH3 [TOKEN AB] | D0 D1 ... D7 | D0 D1 D2 D3 [TOKEN BA] |
| READ | 0x30 [Addr] C0 C1 | D0 D1 ... D15 C0 C1 |
| WRITE (1) | 0xA0 [Addr] C0 C1 | [ACK/NAK] |
| WRITE (2) | D0 D1 ... D15 C0 C1 | [ACK/NAK] |
| INCREMENT (1) | 0xC1 [Addr] C0 C1 | [ACK/NAK] |
| DECREMENT (1) | 0xC0 [Addr] C0 C1 | [ACK/NAK] |
| RESTORE (1) | 0xC2 [Addr] C0 C1 | [ACK/NAK] |
| INC/DEC/RES (2) | D0 D1 ... D15 C0 C1 | [Passive ACK/NAK] |
| TRANSFER | 0xB0 [Addr] C0 C1 | [ACK/NAK] |
| HALT | 0x50 0x00 C0 C1 | [Passive ACK/NAK] |

B CRYPTO1

In this section, we summarize the CRYPTO1 algorithm as reverse-engineered in [25, 12], but do not discuss the numerous vulnerabilities with the cipher which are addressed in the original papers. In the notation of [12], let the (unencrypted) nonce RB be denoted by n_T , the token AB be denoted as $\{n_R\}, \{a_R\}$ and the token BA be denoted as $\{a_T\}$. Also denote by k the key, u the tag's (non) unique identifier (UID), and for any x , let x_i be its i -th bit (when this is well-defined). The CRYPTO1 algorithm uses a Linear Feedback Shift Register (LFSR) of size equal to 48 bits which is initialized by the key (also of length 48). Thus, denoting by $\alpha_i = a_i a_{i+1} \dots a_{i+47}$ the internal state of the LFSR at time i , we get that:

- $a_i := k_i$, for $0 \leq i \leq 47$
- $a_{48+i} := L(a_i, \dots, a_{47+i}) \oplus n_{T,i} \oplus u_i$, for $0 \leq i \leq 31$
- $a_{80+i} := L(a_{32+i}, \dots, a_{79+i}) \oplus n_{R,i}$, for $0 \leq i \leq 31$
- $a_{112+i} := L(a_{64+i}, \dots, a_{111+i})$, $\forall i \in \mathbb{N}$

where L is the LFSR “feedback function” defined by:

$$L(x_0 x_1 \dots x_{47}) := x_0 \oplus x_5 \oplus x_9 \oplus x_{10} \oplus x_{12} \oplus x_{14} \oplus x_{15} \oplus x_{17} \oplus x_{19} \oplus x_{24} \oplus x_{25} \oplus x_{27} \oplus x_{29} \oplus x_{35} \oplus x_{39} \oplus x_{41} \oplus x_{42} \oplus x_{43}$$

The outputs are encrypted using a “filter function”:

$$f(x_0 x_1 \dots x_{47}) := f_c(f_a(x_9, x_{11}, x_{13}, x_{15}), f_b(x_{17}, x_{19}, x_{21}, x_{23}), f_b(x_{25}, x_{27}, x_{29}, x_{31}), f_a(x_{33}, x_{35}, x_{37}, x_{39}), f_b(x_{41}, x_{43}, x_{45}, x_{47})), \text{ where}$$

$$f_a(y_0, y_1, y_2, y_3) := ((y_0 \vee y_1) \oplus (y_0 \wedge y_3)) \oplus (y_2 \wedge ((y_0 \oplus y_1) \vee y_3))$$

$$f_b(y_0, y_1, y_2, y_3) := ((y_0 \wedge y_1) \vee y_2) \oplus ((y_0 \oplus y_1) \wedge (y_2 \vee y_3))$$

$$f_c(y_0, y_1, y_2, y_3, y_4) := (y_0 \vee ((y_1 \vee y_4) \wedge (y_3 \oplus y_4))) \oplus ((y_0 \oplus (y_1 \wedge y_3)) \wedge ((y_2 \oplus y_3) \vee (y_1 \wedge y_4)))$$

These two main functions are summarized in Figure 24.

The keystream bit b_i is then defined by $b_i := f(a_i \dots a_{47+i})$, and the encryption of the i -th regular bit (i.e. excluding start/end and parity bits) is defined by XORing with b_i . Specifically, for $0 \leq i \leq 31$, $\{n_{R,i}\} = n_{R,i} \oplus b_{32+i}$, $\{a_{R,i}\} = a_{R,i} \oplus b_{64+i}$, and $\{a_{T,i}\} = a_{T,i} \oplus b_{96+i}$. Note that the first 32 bits are not used in the first authentication, but they are used in all subsequent authentications, as the tag nonce is encrypted (and the cipher is re-initialized), so that $\{n_{T,i}\} = n_{T,i} \oplus b_i$.

The challenges only depend on the random nonce n_T , with $a_R = \text{suc}^{64}(n_T)$ and $a_T = \text{suc}^{96}(n_T)$, where the “successor function” — also used for the Random Number Generation (RNG) — is iteratively applied 64 and 96 times respectively. It is defined by $\text{suc}(x_0 x_1 \dots x_{31}) := x_1 x_2 \dots x_{31} (x_{16} \oplus x_{18} \oplus x_{19} \oplus x_{21})$ which only depends on the last 16 bits of the input.

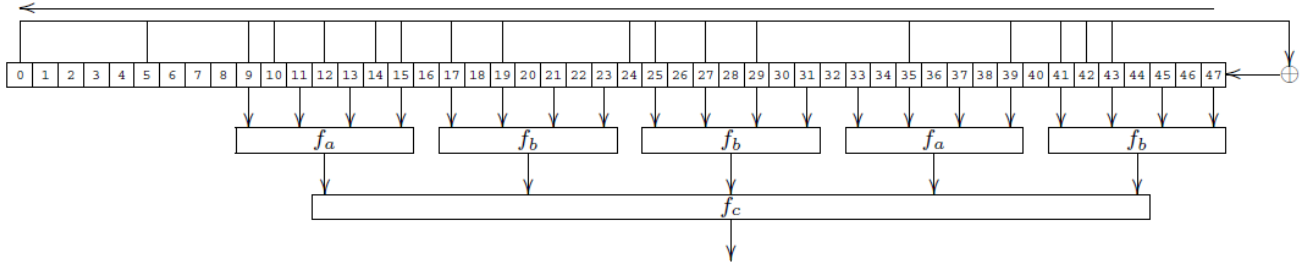


Figure 24. CRYPTO1 LFSR [12]

It is worth noting that the start and ending transmission bits are not encrypted, but the parity bits are — by reusing the encryption bit for the next bit to be encrypted: $\{p_j\} := p_j \oplus b_{8j+8}$. This leaks information, and makes the protocol incompatible with the ISO standard, since the parity bits can be inverted. See Table 8 for an example.

C Example Traces

In this section we show two example traces, one for the MIFARE Ultralight (Table 7) and one for the Classic 1K (Table 8). For the latter, only part of the trace is shown. The key used is 0xFF 0xFF 0xFF 0xFF 0xFF 0xFF, and the exclamation points indicate inverted parity bits.

Table 7. MIFARE Ultralight Trace

| Direction | Bytes | Explanation |
|-----------|---|---|
| PCD→PICC | 0x26 | REQA |
| PICC→PCD | 0x44 0x00 | ATQA |
| PCD→PICC | 0x93 0x20 | ANTICOLLISION (1) |
| PICC→PCD | 0x88 0x04 0xBE 0x6F 0x5D | ANTICOLLISION (1) RESPONSE 0x88 UID0 UID1 UID2 BCC0 $UID0 \oplus UID1 \oplus UID2 \oplus BCC0 = 0x88$ |
| PCD→PICC | 0x93 0x70 0x88 0x04 0xBE 0x6F 0x5D 0xA1 0x8E | SELECT (1) 0x88 + UID[0-2] + BCC0 CRC |
| PICC→PCD | 0x04 0xDA 0x17 | SELECT (1) RESPONSE CRC |
| PCD→PICC | 0x95 0x20 | ANTICOLLISION (2) |
| PICC→PCD | 0x22 0x09 0x29 0x80 0x82 | ANTICOLLISION (2) RESPONSE UID[3-6] + BCC1 $UID3 \oplus UID4 \oplus UID5 \oplus UID6 = BCC1$ |
| PCD→PICC | 0x95 0x70 0x22 0x09 0x29 0x80 0x82 0xD8 0xBA | SELECT(2) UID[3-6] + BCC1 CRC |
| PICC→PCD | 0x00 0xFE 0x51 | SELECT (2) RESPONSE CRC |
| PCD→PICC | 0x30 0x00 0x02 0xA8 | READ ADDR CRC |
| PICC→PCD | 0x04 0xBE 0x6F 0x5D 0x22 0x09 0x29 0x80 0x82 0x48 0x00 0x00 0xE1 0x10 0x12 0x00 0xF8 0x99 | UID UID UID + INTERNAL + LOCK BYTES OTP CRC |
| PCD→PICC | 0x30 0x04 0x26 0xEE | READ ADDR CRC |

| | | |
|----------|---|---|
| PICC→PCD | 0x01 0x03 0xA0 0x10 0x44 0x03 0x00 0xFE 0x00 0x00 0x00 0x00 0x00 0x00 0x00 0x00 0x81 0x3B | USER DATA (1) USER DATA (2) USER DATA (3) USER DATA (4) CRC |
| PCD→PICC | 0x30 0x08 0x4A 0x24 | READ ADDR CRC |
| PICC→PCD | 0x00 0x00 0x00 0x00 0x00 0x00 0x00 0x00 0x00 0x00 0x00 0x00 0x00 0x00 0x00 0x00 0x37 0x49 | USER DATA (1) USER DATA (2) USER DATA (3) USER DATA (4) CRC |
| PCD→PICC | 0x30 0x0C 0x6E 0x62 | READ ADDR CRC |
| PICC→PCD | 0x00 0x00 0x00 0x00 0x00 0x00 0x00 0x00 0x00 0x00 0x00 0x00 0x00 0x00 0x00 0x00 0x37 0x49 | USER DATA (1) USER DATA (2) USER DATA (3) USER DATA (4) CRC |
| PCD→PICC | 0x50 0x00 0x57 0xCD | HALT CRC |

Table 8. MIFARE Classic 1K Trace

| Direction | Plaintext Bytes | Encrypted Bytes | Explanation |
|-----------|--|--|---|
| PCD→PICC | 0x26 | - | REQA |
| PICC→PCD | 0x04 0x00 | - | ATQA |
| PCD→PICC | 0x93 0x20 | - | ANTICOLLISION |
| PICC→PCD | 0xCD 0x76 0x92 0x74 0x5D | - | ANTI RESP UID[0-3] BCC $\oplus UID = BCC$ |
| PCD→PICC | 0x93 0x70 0xCD 0x76 0x92 0x74 0x5D 0x45 0xDD | - | SELECT UID[0-3] + BCC CRC |
| PICC→PCD | 0x08 0xB6 0xDD | - | SELECT RESPONSE CRC |
| PCD→PICC | 0x60 0x3C 0x1A 0x80 | - | AUTH (KEY A) ADDR CRC |
| PICC→PCD | 0x0E 0x61 0x64 0xD6 | - | n_T |
| PCD→PICC | 0x15 0x45 0x90 0xA8 0x4F 0x4E 0x67 0x4E | 0x78 0x5A 0x41 0x80! 0x50! 0x04! 0x8F 0x22! | n_R a_R |
| PICC→PCD | 0x41 0x3E 0xEB 0xCF | 0xCE! 0xCA! 0x0D! 0x83 | a_T |
| PCD→PICC | 0x30 0x3F 0x76 0x61 | 0x69! 0xAC! 0x4F! 0x02 | READ ADDR CRC |
| PICC→PCD | 0x00 0x00 0x00 0x00 0x00 0x00 0xFF 0x07 0x80 0x69 0xFF 0xFF 0xFF 0xFF 0xFF 0xFF 0xD4 0x55 | 0xBC 0x2F 0xBD! 0xB1! 0x75! 0x44! 0x3C 0xD7! 0xD2 0x28 0x3B! 0xA5! 0x08 0x04 0x88! 0x18! 0x89 0x42! | KEY A (INACCESSIBLE) ACCESS BITS KEY B CRC |

| | | | |
|----------|---|--|---|
| PCD→PICC | 0x30 0x3E 0xFF 0x70 | 0x71! 0xF7 0x9F! 0x31 | READ ADDR CRC |
| PICC→PCD | 0x00 0x00 0x00 0x00 0x00 0x00 0x00 0x00 0x00 0x00 0x00 0x00 0x00 0x00 0x00 0x00 0x37 0x49 | 0xE2! 0x99! 0x8D 0xE0 0x3F 0x96! 0xEF 0xC5 0xD0 0xD3! 0x24! 0x87! 0xF7 0x15! 0x06! 0x55! 0xA0! 0x97! | USER DATA (1) USER DATA (2) USER DATA (3) USER DATA (4) CRC |
| PCD→PICC | 0x30 0x3D 0x64 0x42 | 0xC1! 0x43 0x22!0x92! | READ ADDR CRC |
| PICC→PCD | 0x00 0x00 0x00 0x00 0x00 0x00 0x00 0x00 0x00 0x00 0x00 0x00 0x00 0x00 0x00 0x00 0x37 0x49 | 0xD2 0x00! 0x9D 0x87! 0xD9 0x0D 0x25 0x73 0x51 0x27 0x44 0xCC! 0x55 0x44! 0x85 0x9D 0x44 0xF6 | USER DATA (1) USER DATA (2) USER DATA (3) USER DATA (4) CRC |
| PCD→PICC | 0x30 0x3C 0xED 0x53 | 0x27 0x02 0x5C 0x41! | READ ADDR CRC |
| PICC→PCD | 0x00 0x00 0x00 0x00 0x00 0x00 0x00 0x00 0x00 0x00 0x00 0x00 0x00 0x00 0x00 0x00 0x37 0x49 | 0x8B! 0xD1! 0xE3 0x87! 0x63! 0x75! 0x44 0x34 0x3B 0xAF! 0x27 0x0A! 0xAD! 0x84 0x1C 0xDB! 0xD8 0x4A | USER DATA (1) USER DATA (2) USER DATA (3) USER DATA (4) CRC |
| PCD→PICC | 0x60 0x38 0x3E 0xC6 | 0xC6 0xDC 0xBA! 0x11! | (NESTED) AUTH (KEY A) ADDR CRC |
| PICC→PCD | 0x8F 0x82 0x69 0x9E | 0x70! 0xBD 0xED! 0x81 | (ENCRYPTED) n_T |
| PCD→PICC | 0x01 0x3A 0x6B 0xBA 0x73 0xD4 0x42 0x2D | 0xFC! 0x1A 0x1A! 0x1D! 0x7D! 0x90 0x7E! 0x24! | n_R a_R |
| PICC→PCD | 0xD0 0xA2 0x28 0xDB | 0x87 0x4D 0xFF! 0x8A | a_T |
| PCD→PICC | 0x30 0x3B 0x52 0x27 | 0x31 0x56 0xA1! 0x84 | READ ADDR CRC |
| PICC→PCD | 0x00 0x00 0x00 0x00 0x00 0x00 0xFF 0x07 0x80 0x69 0xFF 0xFF 0xFF 0xFF 0xFF 0xFF 0xD4 0x55 | 0x64 0x85! 0x16 0x6D 0xCF! 0xF7 0x3C! 0x62 0xD2 0xB4 0x3B! 0x5F! 0xA8! 0x71 0xD1 0x6B! 0x6C! 0x42 | KEY A (INACCESSIBLE) ACCESS BITS KEY B CRC |
| PCD→PICC | 0x30 0x3A 0xDB 0x36 | 0x02! 0x44! 0xD4! 0x47! | READ ADDR CRC |
| PICC→PCD | 0x00 0x00 0x00 0x00 0x00 0x00 0x00 0x00 0x00 0x00 0x00 0x00 0x00 0x00 0x00 0x00 0x37 0x49 | 0x41 0xBC! 0x42! 0xD9 0x39 0x4C! 0x9A 0x80! 0x4E 0x76 0xB1! 0xA1! 0xA4 0xD1 0x82! 0x61 0x28 0xBC! | USER DATA (1) USER DATA (2) USER DATA (3) USER DATA (4) CRC |
| PCD→PICC | 0x30 0x9 0x40 0x04 | 0xA5 0x63 0x90! 0x32! | READ ADDR CRC |
| PICC→PCD | 0x00 0x00 0x00 0x00 0x00 0x00 0x00 0x00 0x00 0x00 0x00 0x00 0x00 0x00 0x00 0x00 0x37 0x49 | 0xBD! 0xC3 0xA6! 0x15 0x8B 0x2A! 0x6A! 0x03 0x72! 0xEF! 0x02! 0x38 0x05! 0xC5! 0x3F 0x4E! 0x94! 0x08 | USER DATA (1) USER DATA (2) USER DATA (3) USER DATA (4) CRC |

| | | | |
|----------|---|---|---|
| PCD→PICC | 0x30 0x38 0xC9 0x15 | 0xE2 0x1C! 0x8A 0x16! | READ ADDR CRC |
| PICC→PCD | 0x00 0x00 0x00 0x00 0x00 0x00 0x00 0x00 0x00 0x00 0x00 0x00 0x00 0x00 0x00 0x00 0x37 0x49 | 0x51 0x1B 0xA6! 0x49 0x29! 0xF2 0x75 0x35! 0x1B! 0xE1 0x72 0x68 0x7F 0x3F 0x2A 0xE9! 0x73 0x0F | USER DATA (1) USER DATA (2) USER DATA (3) USER DATA (4) CRC |
| PCD→PICC | 0x60 0x34 0x52 0x0C | 0x7F! 0xB8! 0x88 0x7B! | (NESTED) AUTH (KEY A) ADDR CRC |
| PICC→PCD | 0xDC 0xFC 0x96 0x2B | 0x23! 0x23! 0x6E 0xF4! | (ENCRYPTED) n_T |
| PCD→PICC | 0xEE 0x08 0xB0 0x0A 0xF6 0x01 0xBA 0x11 | 0x1A 0xB9! 0xEF! 0x7B! 0xC5 0xC3 0x51 0x57! | n_R a_R |
| PICC→PCD | 0x6E 0x27 0x63 0x93 | 0x3E 0x19 0x48! 0xF4! | a_T |
| PCD→PICC | 0x30 0x37 0x3E 0xED | 0xD6! 0x59! 0xB4! 0x73! | READ ADDR CRC |
| PICC→PCD | 0x00 0x00 0x00 0x00 0x00 0x00 0xFF 0x07 0x80 0x69 0xFF 0xFF 0xFF 0xFF 0xFF 0xFF 0xD4 0x55 | 0x32! 0x84 0xE6 0xB1! 0x45! 0x56! 0x5C! 0x1A! 0xED! 0xD3! 0xED! 0x76 0x32! 0x5F 0x5D! 0x4D 0x96! 0xFC! | KEY A (INACCESSIBLE) ACCESS BITS KEY B CRC |
| PCD→PICC | 0x30 0x36 0xB7 0xFC | 0xBB! 0x4D! 0xF8 0x55 | READ ADDR CRC |
| PICC→PCD | 0x00 0x00 0x00 0x00 0x00 0x00 0x00 0x00 0x00 0x00 0x00 0x00 0x00 0x00 0x00 0x00 0x37 0x49 | 0x7E 0x9E! 0x34! 0x38! 0xDC! 0xE2! 0xF9 0x98! 0xA0 0x88 0x78! 0xA9! 0xCD! 0xEE! 0x17 0xD8 0xFF! 0xFD! | USER DATA (1) USER DATA (2) USER DATA (3) USER DATA (4) CRC |